

Fuzzy PD+I hybrid controller for load frequency control

Arishnil Bali* and Utkal Mehta

School of Engineering and Physics, The University of the South Pacific, Laucala Campus, Fiji. E-mail: utkal.mehta@usp.ac.fj

To supply good quality power, the Load frequency control (LFC) acts an important role toward the system uncertainty and disturbance elimination capability for both isolated and interconnected power systems. The fuzzy based controller has the properties such as, controlling the overshoot and rise time of the response whereas the conventional controller reduces the steady state error quickly. This makes the hybrid control actions quite suitable for the LFC. Therefore, in this work a fuzzy hybrid technique is designed to generate the controller action. Initially, the hybrid approach is tested on a single area LFC for two turbine types i.e., non-reheated and reheated and then it is extended to multi-area cases. It is observed that the proposed controller displays better robustness toward $\pm 50\%$ parametric uncertainty and disturbance rejection capability as compared to the existing techniques

Keywords: Load frequency control; Hybrid controller; Multi-area power systems; Disturbance rejection; Perturbations

1. INTRODUCTION

In power systems, natural energy is converted to electrical energy, and thus optimization of electrical equipment is necessary for superior output. It is also required to maintain both the voltage and frequency at a fixed desired value regardless of the change in loads, however, without any control, it is quite impossible to maintain the active and reactive power from varying [1]. To solve this issue, a control is needed in the system. Monitoring and controlling the real power generated within specified limits in response to changes in system frequency and tie-line power interchange is known as load frequency control (LFC). The key role of LFC is to retain the frequency at a desired constant value against the fluctuating active power loads.

Several units make up an interconnected power system in a large scale power system and therefore both constant fre-

quency and constant tie-line power exchange should be provided for the stable operation of power systems. Automatic Generation Controller (AGC) calculates the alteration in the generation (Area Control Error - ACE) by taking note of system frequency and tie-line flows, and thus, retains the time average of the ACE at a minimum value within the area by adjusting the set position of the generators [1].

Several strategies for LFC in various power systems have been presented by researchers as to retain the system frequency and tie-line flow at their assigned values throughout their regular process and also during slight perturbations. An acute literature review on the AGC of power systems was presented by Ibraheem and Kothari [2] where various recent philosophies of control aspects have been studied. Moreover numerous control techniques have been proposed to address the LFC over the past decade [3-15, 23-25]. These include using genetic algorithm, differential evolution, fuzzy controller, hybrid evolutionary fuzzy PI controller, bacteria foraging optimization algorithm. Recently, unified IMC PID tuning [15]

*Corresponding Author. E-mail: s11068975@student.usp.ac.fj

and new control scheme using Laurent series [16] have presented to improve the load disturbance rejection performance. Certainly, PI/PID controllers for LFC were studied due to their simplicity in execution. The fuzzy controlled applications are rapidly increasing in industry today due to the easily interpretable form of the controller rule base which makes the tuning procedure more effortless. References [6], [17-23] suggested adaptive fuzzy or neural base controllers for load frequency control of power systems. It has been proved in literature to reveal the fact that fuzzy logic may at times be a better approach in designing controllers for various systems over the classical linear PID controllers as it has been verified for its robustness and being less sensitive to parametric variations.

A new Fuzzy PD plus I (FPD+I) hybrid controller is presented, the mixture of a fuzzy logic controller and a conventional controller. In this way, the fuzzy based PD action plays a significant role in controlling the rise time and overshoot of the response whereas the conventional integral action reduces the steady state error quickly. The presented design leads to significant control enhancements, particularly for system perturbation and disturbance rejection. Furthermore, the merit of the given design method is presented by comparing the proposed method with few lately published methods.

2. SINGLE AREA POWER SYSTEM MODEL

The main aim of power systems is to generate and supply power to its customers. With the growing demand of power supplies in domestic and industrial areas, power has to be constantly supplied without any disturbance. However, there are many factors that cause hindrance in the supply of power. One major problem faced in power system is the fluctuating load demand. In the case of the LFC, the power system considered is taken to have little variations in the load. Thus, this could appropriately be demonstrated by the linear model and so linearizing around the operating point. Moving on, a single area power system contains a turbine, load and machines, a governor and also droop characteristics (a kind of feedback gain included in the power system that improves the damping properties). Fig. 1 shows a single area power system as a linear model [15], where a single generator is used to supply power to a single area.

Table 1 shows the nomenclature of the various parameters being used in the system. The transfer function model with droop characteristics of the overall system can be represented as [15, 16]:

$$G(s) = \frac{G_g(s)G_t(s)G_p(s)}{1 + G_g(s)G_t(s)G_p(s)/R} \quad (1)$$

where

$$\frac{1}{R} = \text{droop characteristics}, \quad (2)$$

$$G_g(s) = \text{Governor dynamics} := \frac{1}{T_{G^{s+1}}}.$$

$$\text{Case-1 : Non-reheated turbine: } G_t(s) = \frac{1}{T_{I^{s+1}}} \quad (3)$$

ΔP_d Load disturbance (p.u. MW)

K_P Electric system gain

T_P Electric system time constant (s)

T_T Turbine time constant (s)

T_G Governor time constant (s)

R Speed regulation due to governor action (Hz/p.u. MW)

T_x Constant of reheat turbine

c % of power generated in the reheat portion

Δf Incremental frequency deviation (Hz)

ΔP_G Incremental change in generator o/p (p.u.MW)

ΔX_G Incremental change in governor valve position

ΔP_{tie} Tie-line power change (p.u.MW)

T_{ij} Synchronizing constant

B_i Frequency bias constant

$$\text{Case-2: Reheated turbine: } G_t(s) = \frac{cT_{I^{s+1}}}{(T_{I^{s+1}})(T_{I^{s+1}})} \quad (4)$$

$$G_p(s) = \text{Load and machine dynamics} := \frac{K_P}{T_{P^{s+1}}} \quad (5)$$

After substituting (2–5) in the system model (1), one can obtain the model as:

$$G(s) = \frac{K_P}{(T_{P^{s+1}})(T_{T^{s+1}})(T_{G^{s+1}}) + K_P/R} \quad (6)$$

Hydro turbine or a steam turbine might have been used as the type of turbine in the system. Two types of steam turbine are considered in this current work, Reheat Turbine (RT) and Non-Reheat Turbine (NRT). Let's take into consideration a power system with a NRT and a RT proposed in [15, 16].

The model parameters are:

1. Non-Reheated Turbine: $K_P = 120, T_P = 20, T_T = 0.3, T_G = 0.08, R = 2.4.$

2. Reheated Turbine: $K_P = 120, T_P = 20, T_T = 0.3, T_G = 0.08, R = 2.4, T_r = 4.2, c = 0.35.$

3. FUZZY PD PLUS I HYBRID DESIGN

In this section, the new Fuzzy PD plus I (FPD+I) controller technique is illustrated. Let's take first the linear conventional PID in parallel form and its transfer function written as:

$$C(s) = \frac{U(s)}{E(s)} = K_c + \frac{K_i}{s} + K_d s \quad (7)$$

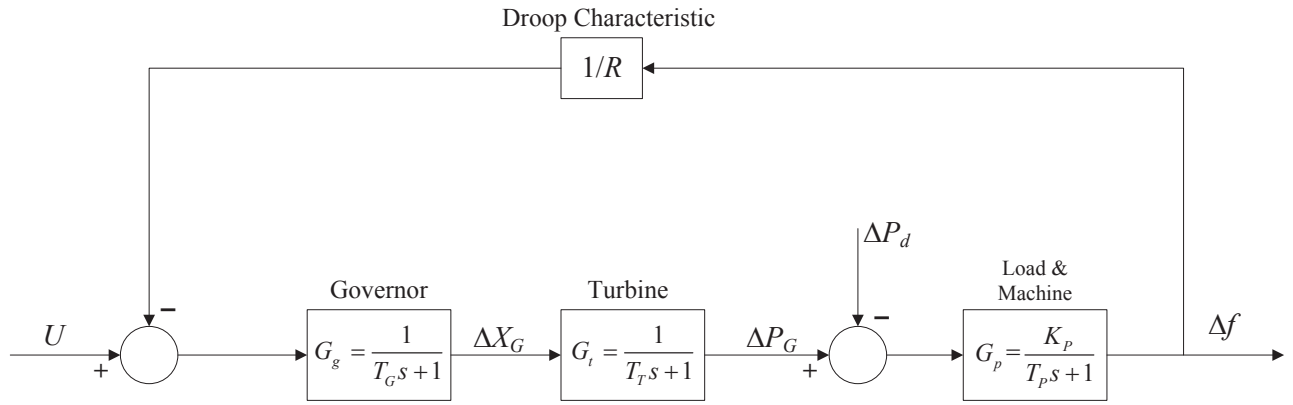


Figure 1 A single area power system.

where K_c , K_i and K_d are the proportional, integral and derivative gains respectively.

This can be written in a continuous time domain is:

$$U(t) = K_c + K_i \int_0^t E(t)dt + K_d \frac{dE(t)}{dt} \quad (8)$$

The proposed technique of hybrid controller maintains the same linear structure of the PID parts, however, it contains constant coefficient yet self-tuned control gains. The scheme consists of fuzzy logic but is included only for the design as the fuzzy rule base doesn't need to be executed, and thus, it is in fact a conventional PID controller with analytic formulas. The foremost enhancement is in providing the classical controller with adaptive control capability up to a certain limit. However, it is important to estimate the optimal PID gains with specified robustness. Then after the fuzzy PD gains are computed from the output error and the change in error.

3.1 Optimal PID gains based on constraint

Many different approaches exist to find the optimal PID gains. The simplest way deals with the use of open-loop transfer function for guaranteed robust performance. Wang and Shao [16] have proposed a robustness index λ such that the Nyquist curve of the loop transfer function is tangent to a line parallel to the imaginary axis in the left-half of the complex plane and it is defined as:

$$\frac{1}{\lambda} = \max_{0 < \omega < \infty} |\operatorname{Re}[C(j\omega)G(j\omega)]| \quad (9)$$

where:

the quantity λ is simply the inverse of maximum of absolute real part of loop transfer function.

Based on the constraint imposed on the integrated error criterion, the optimal controller tuning formulae are suggested as

$$K_c = \frac{1}{\lambda \alpha'(\omega_{90})} \left(\frac{\beta'(\omega_{90})}{\beta(\omega_{90})} - \frac{1}{\omega_{90}} \right) \quad (10)$$

$$K_i = -\frac{\omega_{90}}{\lambda \beta(\omega_{90})} \quad (11)$$

If these tuning rules are extended using standard relation of integral and derivative gain constants, one can derive relation

for derivative gain as:

$$K_d = \frac{K_c^2}{4K_i} \quad (12)$$

Here, $\alpha(\omega_{90})$ and $\beta(\omega_{90})$ are the real and imaginary parts of the process transfer $G(j\omega)$. The frequency ω_{90} is the point when the Nyquist curve touches the imaginary axis.

3.2 Transferring gains from PID to fuzzy

The aim is to transfer optimal values of the linear PID gains to the nonlinear fuzzy controller. In this control technique, a fuzzy logic controller for proportional-derivative actions and a conventional controller for integral action are combined in the FPD+I controller. Basically, the error predicted through the derivative action, hence, the PD controller utilizes this derivative action in improving closed-loop stability. Input of FPD has the error (E) and the change in error (DE), as shown in Fig. 2. In crisp PD terms, it is also called derivative of the error.

Now, the nonlinear fuzzy function gives the controller output from inputs, *error* and *change in error* as:

$$U_n = [f(GP * e_n, GD * de_n)] * GU \quad (13)$$

By adding an integral action as shown in Fig. 2, the overall controller output can be written as:

$$U = [f(GP * e_n, GD * de_n)] * GU + GI * ie_n \quad (14)$$

Using linear approximation as suggested in [19], the controller output is obtained as:

$$\begin{aligned} U &= [GP * e_n + GD * de_n] * GU + GI * ie_n \\ &= [GP * GU * e_n + GD * GU * de_n] + GI * ie_n \end{aligned} \quad (15)$$

It is assumed to be non-zero GU and after comparing (8) and (13), the controller gains are related in the following way:

$$\begin{aligned} GP &= \frac{K_c}{GU} \\ GD &= \frac{K_d}{GU} \\ GI &= K_i \end{aligned} \quad (16)$$

In order to obtain a kind of nonlinear fuzzy advantage, the internal structure of fuzzy controller is designed as described below.

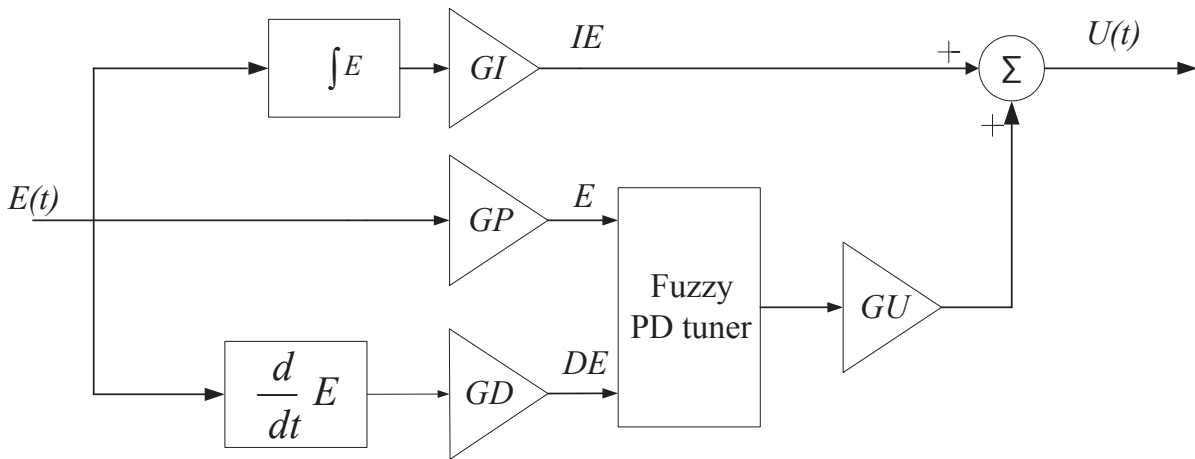


Figure 2 Controller structure Fuzzy PD plus I.

3.3 Designing nonlinear fuzzy PD action

The FPD controller used in this paper has a standard structure, consisting of a Fuzzy Rule Base (*FRB*), Parameter Base (*PB*) and a Computational Unit (*CU*) that performs the following three basic operations: *Fuzzyfication*, *Fuzzy Inference* and *Defuzification* as in [20–22].

The Parameter Base contains the parameters of all pre-defined *Membership Functions* for both inputs of the FPD, namely: the *Error* and *Change-of-Error*. Here, equal number of 7 membership functions is assumed to represent the respective *Linguistic Variables* for both inputs, as follows:

Negative Large (*NL*), Negative Medium (*NM*), Negative Small (*NS*), Positive Small (*PS*), Zero (*ZR*), Positive Medium (*PM*) and Positive Large (*PL*).

Triangular shape for all membership functions of the FPD+I controller was assumed, as it is the case in most fuzzy control applications [21, 23]. As for the *centers* of the membership functions they have been predefined to be located at equal distances within the *normalized range* $[-1, +1]$ for the Error and Change of the Error, as follows:

NL at -1.0 ; *NM* at -0.66 ; *NS* at -0.33 ; *ZR* at 0.0 ; *PS* at $+0.33$; *PM* at $+0.66$ and *PL* at $+1.0$.

All pairs of neighboring membership functions, for example: *NL* and *NM*, *ZR* and *PS*, *PS* and *PL* etc. have maximal overlapping value of 0.5 at their cross point and they do not overlap with any other (not neighboring) membership functions.

In general, the fuzzy rules of the Mamdani-type fuzzy controller [21, 23] have the following entirely linguistic structure:

IF (*Error* is {*LV*} and *Change-of-Error* is {*LV*})
THEN *Change-of-Output* is {*LV*}

Here {*LV*} represents a linguistic variable taken from the pre-defined list of linguistic variables for the *Error*, *Change-of-Error* and *Change-of-Output*.

In this paper, the Takagi-Sugeno-type (TS) fuzzy controller [22] is used, which differs from Mamdani-type controller in the *consequent* part of the rules, namely that they are now represented not linguistically, but by crisp numerical values,

Table 1 The Fuzzy Rule Base of the proposed FPD+I controller.

Change of Error	PL	ZR	PS	PS	PM	PL	PL	PL
	PM	NS	ZR	PS	PM	PM	PM	PL
	PS	NM	NS	ZR	PS	PS	PM	PL
	ZR	NL	NM	NS	ZR	PS	PM	PL
	NS	NL	NM	NS	NS	ZR	PS	PM
	NM	NL	NM	NM	NM	NS	ZR	PS
	NL	NL	NL	NL	NM	NS	NS	ZR
Error	NL	NM	NS	ZR	PS	PM	PL	

known as *singletons* [22]. The following values for all 7 singletons in the proposed FPD+I controller have been assumed: *NL* is -1.0 ; *NM* is -0.66 ; *NS* is -0.33 ; *ZR* is 0.0 ; *PS* is $+0.33$; *PM* is 0.66 and *PL* is $+1.0$.

Under the above design assumptions, the fuzzy rule base of the FPD+I controller consists of $7 \times 7 = 49$ fuzzy rules. They have been created in the form of linguistic decisions about the amount of the *change-of-output* of the controller for each combination of *Error* and *Change-of-Error*. These are common-sense decisions that a control engineer would make for each situation, based on his previous control experience. The FRB for the proposed FPD+I controller is given in Table 2.

The control surface for assumed rule based is shown in Fig. 3, based on all assumed parameters for the membership functions and singletons. The calculations for the response surface of the FPD+I controller have been done by using *product* operation as inference step and *weighted average* as defuzzification step [21–23].

A comparison between the responses surface of linear PD and proposed fuzzy reveals immediately the difference between the linear and nonlinear behaviour (reaction) of the controllers. The nonlinear behaviour of FPD has the potential benefit to be more flexible and resilient in reacting to different type of disturbances, subject to a “proper tuning” of all its internal parameters, compared to the linear PD controller. This is demonstrated in the sequel of the paper by various simulations.

The number of all internal parameters of FPD+I

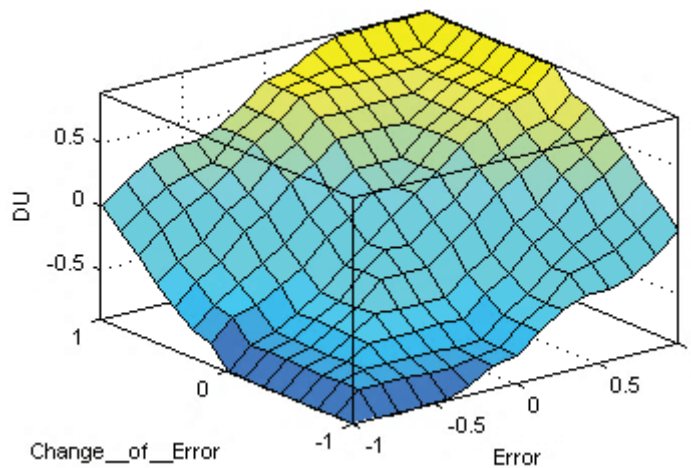


Figure 3 Control surface for rule base.

controller that should be tuned for its optimal performance is usually large and grows rapidly with increasing the number of the membership functions that are used in generating the fuzzy rules in the FRM. For example, for this assumed design structure of the FPD+I controller, there are 21 parameters to be tuned as follows: 7 locations (centers) for the membership functions of the input: *Error*; 7 centers for the membership functions of the input: *Change-of-Error* and another portion of 7 parameters $\hat{\Delta}$ “the singletons for the outputs of the fuzzy rules.

In order to optimize all these 21 parameters, a reliable optimization method and algorithm is needed that is able to find the global optimum, without being stalled at some of the numerous local optimums. The solution of this task goes beyond the scope of this paper. A rough adjustment is made to the parameter values of FPD+I controller in a “reasonable” way which mostly relied on the “fuzzy logic power” of the fuzzy rule base that is able to apply proper and robust control actions. Therefore, instead of fine tuning of all 21 parameters of FPD+I controller, the three “external” parameters $\hat{\Delta}$ “the above scaling factors *GP*, *GD* and *GI* in (15) has only been tuned.

It is obvious that if fine tuning of the whole group of parameters of FPD+I controller is done, its performance will definitely increase.

4. SIMULATION RESULTS FOR SINGLE AREA SYSTEM

The simulation results obtained for both nominal and uncertain cases are presented for the proposed FPD+I hybrid controller. Table 3 shows the FPD+I controller parameters settings for all types of turbines models. It is seen that the hybrid technique, in both the types of turbines, provide an improved response for the nominal and for the uncertain case.

Figs. 4 and 5 show the responses attained by employing the presented method to the nominal Non-Reheated Turbine power systems. Adding on, a load demand of $\Delta P_d = 0.1$ is being added to the system at time 1 s. From the figures

obtained, it is observed that the hybrid approach provides the quickest disturbance rejection than the method presented by Padhan and Majhi [16].

Table 2 Controller settings for single area system.

Power system models	FPD+I settings with GU=10
NRTWD	$GP=0.20, GD=0.14, GI=1.67$
NRTD	$GP=0.20, GD=0.06, GI=1.67$
RTWD	$GP=0.76, GD=0.49, GI=5.85$
RTD	$GP=0.60, GD=0.24, GI=2.14$

NRTWD: Non-Reheat Turbine Without Droop, NRTD: Non-Reheat Turbine with Droop, RTWD: Reheat Turbine Without Droop, RTD: Reheat Turbine with Droop.

Noted that the superior performance was recorded in [16] as compared to the internal model control based PID designed by Tan [15]. Hence it is evident that the new FPD+I controller at present achieves much greater compared to the methods suggested by Tan [15]. To examine the robustness of the FPD+I controller, the parameter variations of the system are taken as $\pm 50\%$ of their nominal values.

In this case also, parametric uncertainty is included in the system, together with a 0.1 disturbance at time 1 s. It is observed from Figs. 3 and 4 that the suggested hybrid controller has a better performance in disturbance rejection as compared to the existing techniques under uncertain environment.

Likewise, similar results were achieved for the Reheated Turbine power system. Figs. 6 and 7 shows the responses attained for the Reheated Turbine with and without droop for nominal along with uncertain cases.

It is evident from the results obtained through simulation that the characteristics of the FPD+I controller enables it to be reliable and appropriate for the LFC. Knowing the fact that the key role of the LFC is to monitor and control the fluctuations in frequency taking place even if the parameters aren't constant in the power system.

The fluctuations occurring in the power system are represented by introducing the disturbances whilst varying $\pm 50\%$ in different parameters signifies the parametric uncertainty taking place in the system. Finally, the proposed nonlinear

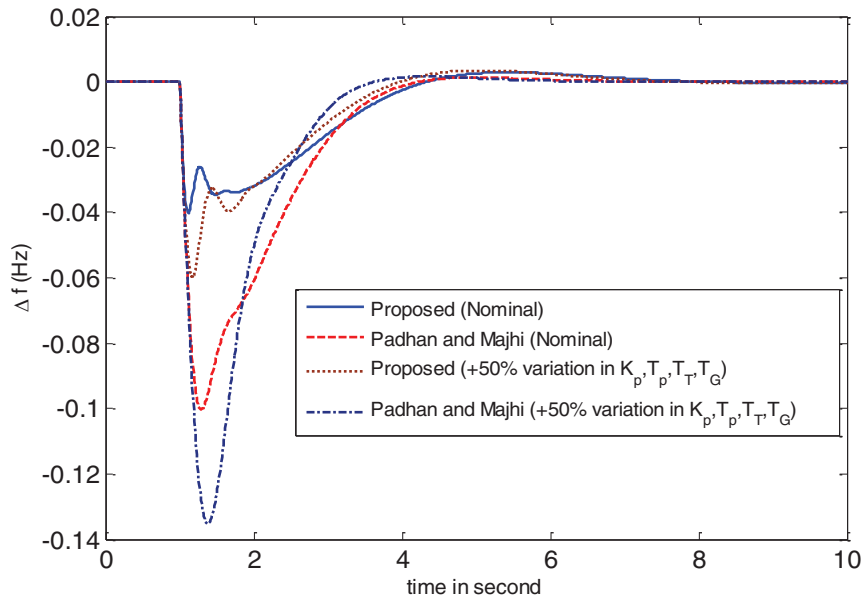


Figure 4 Frequency deviation for NRTWD.

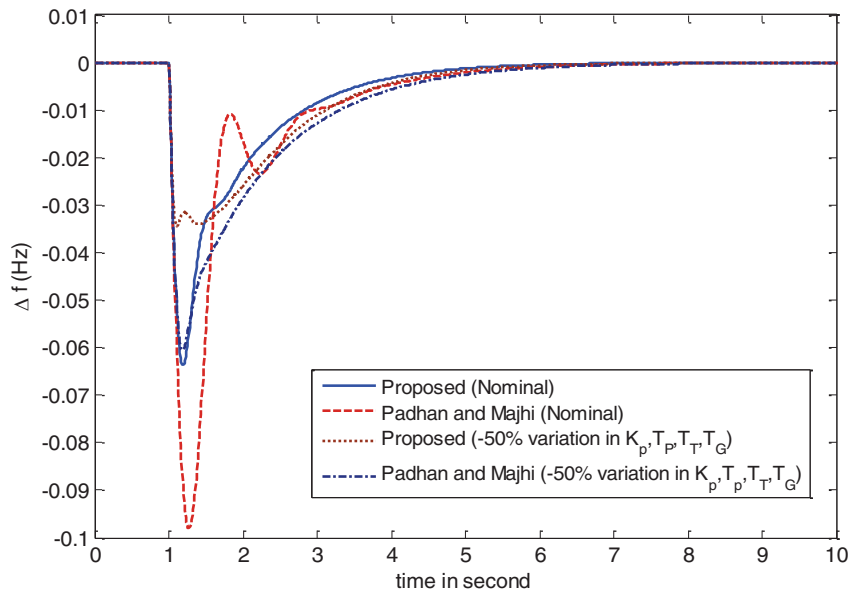


Figure 5 Frequency deviation for NRTD.

controller obtains reduced settling time and overshoot as compared to the existing control techniques in the literature.

5. CONTROL OF MULTI-AREA POWER SYSTEM

Areas interconnected by means of high voltage transmission lines or tie-lines are referred to as a multi-area power system. The behaviour of frequency noted in each control area reflects the behaviour of the mismatch power in the interconnection and not in the control area alone [16]. Moving on, variations in area frequency and tie-line power interchange occur as power load demand randomly varies in situations of a decentralized power system.

The main goal of a decentralized LFC is to reduce the tran-

sient deviations of such variables and to make certain that their steady state errors become zero. Unpredicted external disturbances along with parameter and model uncertainties pose a huge challenge in designing the controller when operating with the LFC problem of power systems. For N control areas (Fig. 8), the total tie-line power change between area 1 and other areas is given as:

$$\Delta P_{tie1} = \sum_{\substack{j=1 \\ j \neq 1}}^N \Delta P_{tie1j} = \frac{1}{s} \left[\sum_{\substack{j=1 \\ j \neq 1}}^N T_{ij} \Delta f_i - \sum_{\substack{j=1 \\ j \neq i}}^N T_{ij} \Delta f_j \right] \quad (17)$$

By means of identifying the frequency and tie-line power deviations to generate the ACE signal, the steadiness amongst

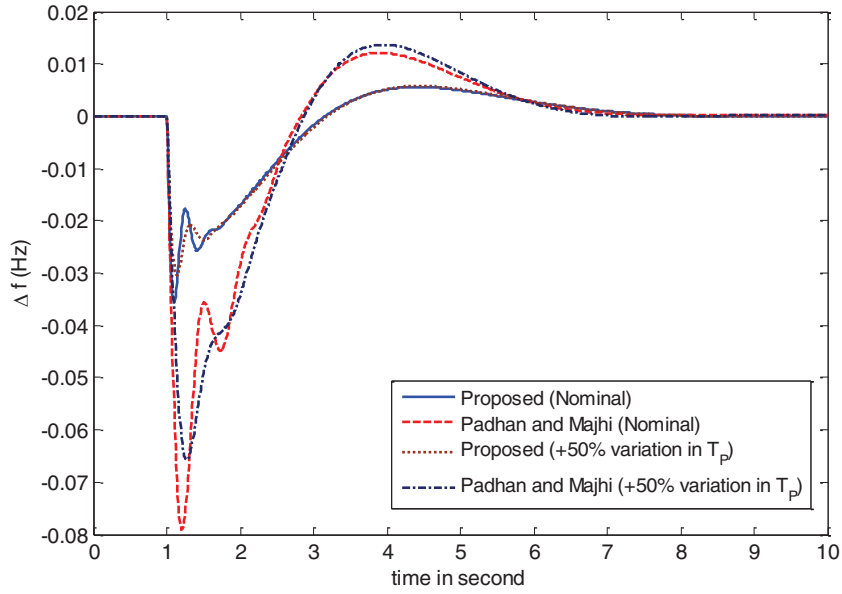


Figure 6 Frequency deviation for RTWD.

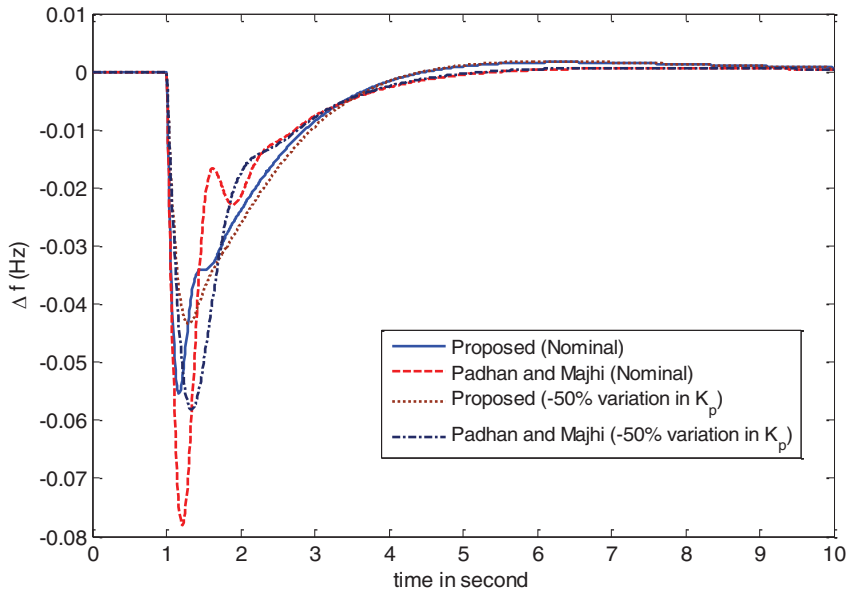


Figure 7 Frequency deviation for RTD.

connected control areas is obtained, which then rather is employed in the control strategy as presented in Fig. 8 [16]. Adding on, linear combination of tie-line power change and frequency deviation can be used to express the ACE for each control area.

$$ACE_i = B_i \Delta f_i + \Delta P_{tiei} \quad (18)$$

The Load Frequency Control system in each control area of an interconnected (multi-area) power system should control the interchange power with the other control areas along with its local frequency. The generalized system transfer function for multi-area power system is given by:

$$G_i(s) = B_i \frac{G_{gi}(s)G_{ti}(s)G_{pi}(s)}{1 + G_{gi}(s)G_{ti}(s)G_{pi}(s)/R_i} \quad (19)$$

Now, the FPD+I hybrid controller can be designed based on the individual area's transfer function in (18) and following the same procedure discussed in Section 3.

5.1 Simulation results for 4 area power system

Fig. 9 shows a simplified 4 area interconnected power system that was taken for this study. Let's consider the interconnected four area power system with one NRT and three RT studied in [15, 16].

The model parameters are:

1. Area 1, 2 and 3 reheated turbines: $K_{P1} = K_{P2} = K_{P3} = 120$, $T_{P1} = T_{P2} = T_{P3} = 20$, $T_{T1} = T_{T2} = T_{T3} = 0.3$, $T_{G1} = T_{G2} = T_{G3} = 0.2$, $R_1 = R_2 = R_3 =$

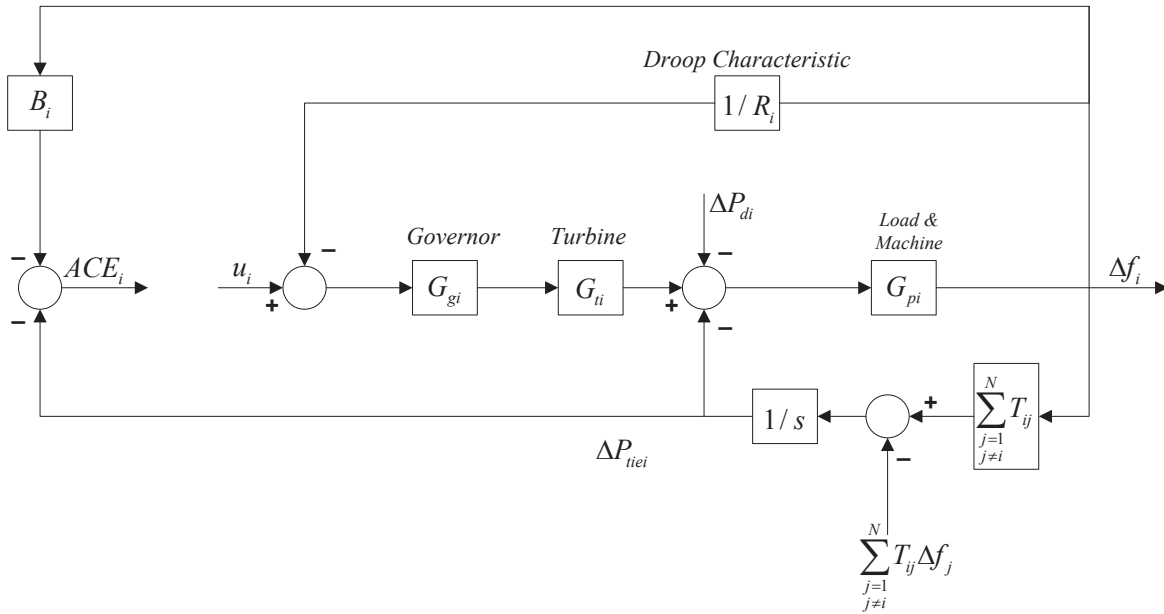


Figure 8 Block diagram representation of control area i .

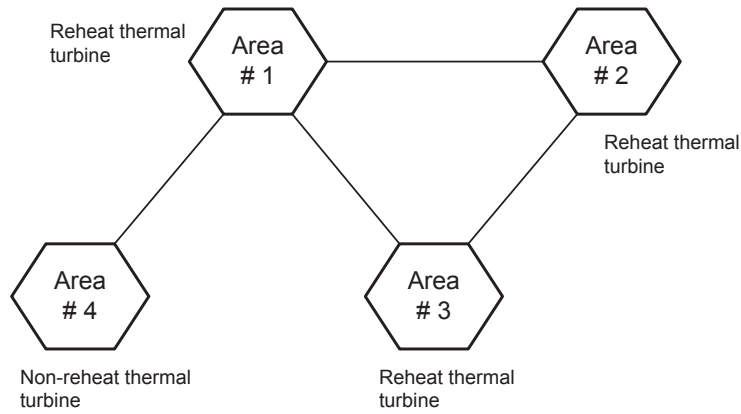


Figure 9 Simplified interconnected power system diagram.

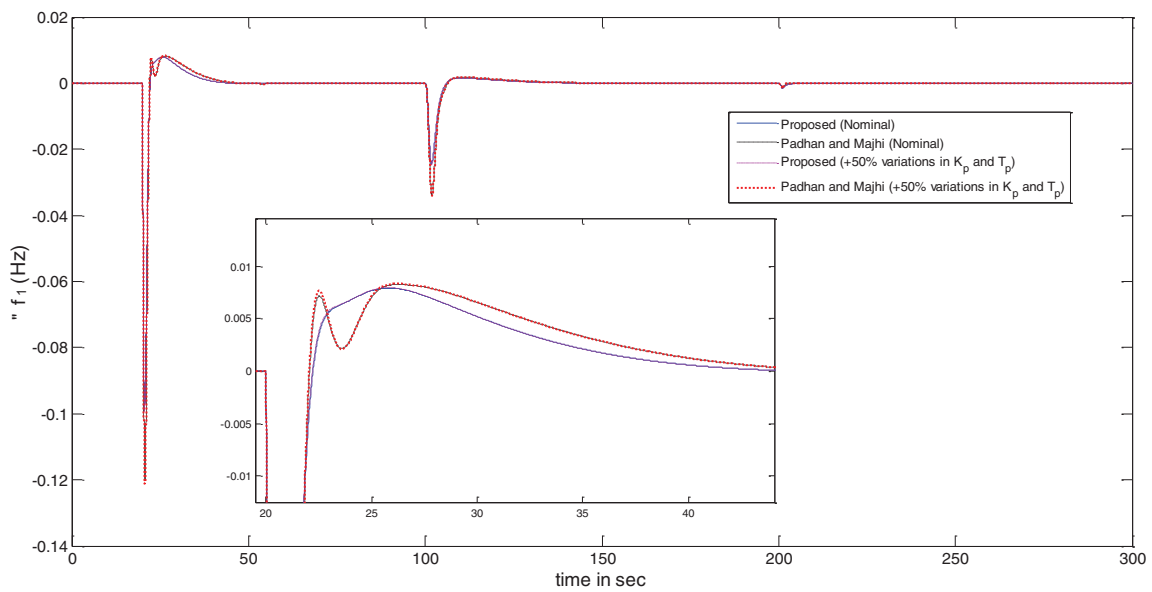


Figure 10 Frequency deviation in area 1 following a small change in loads ΔP_{di} .

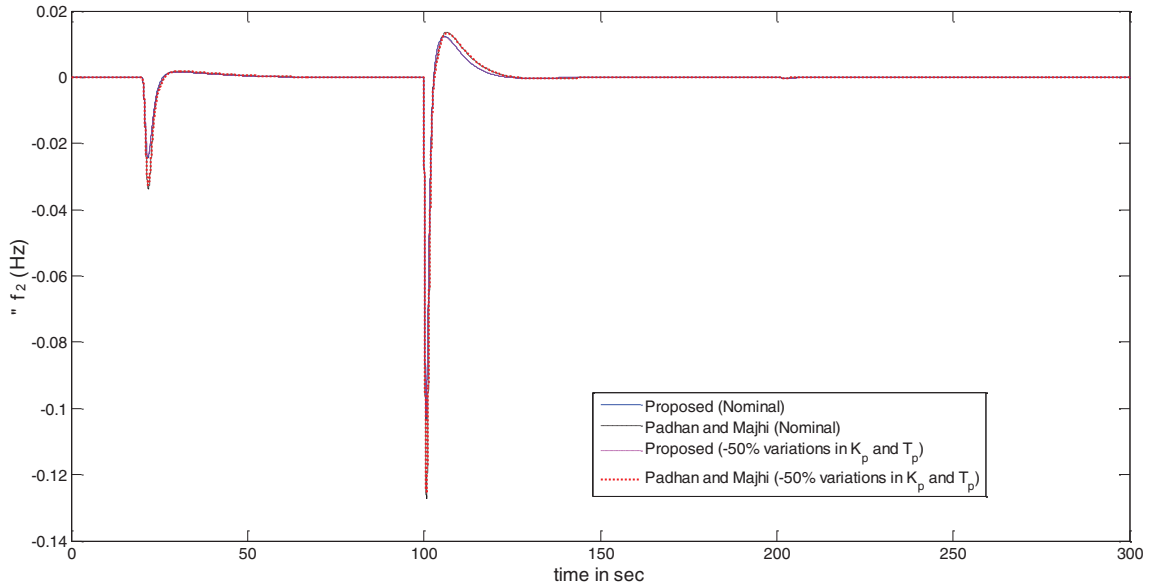


Figure 11 Frequency deviation in area 2 following a small change in loads ΔP_{di} .

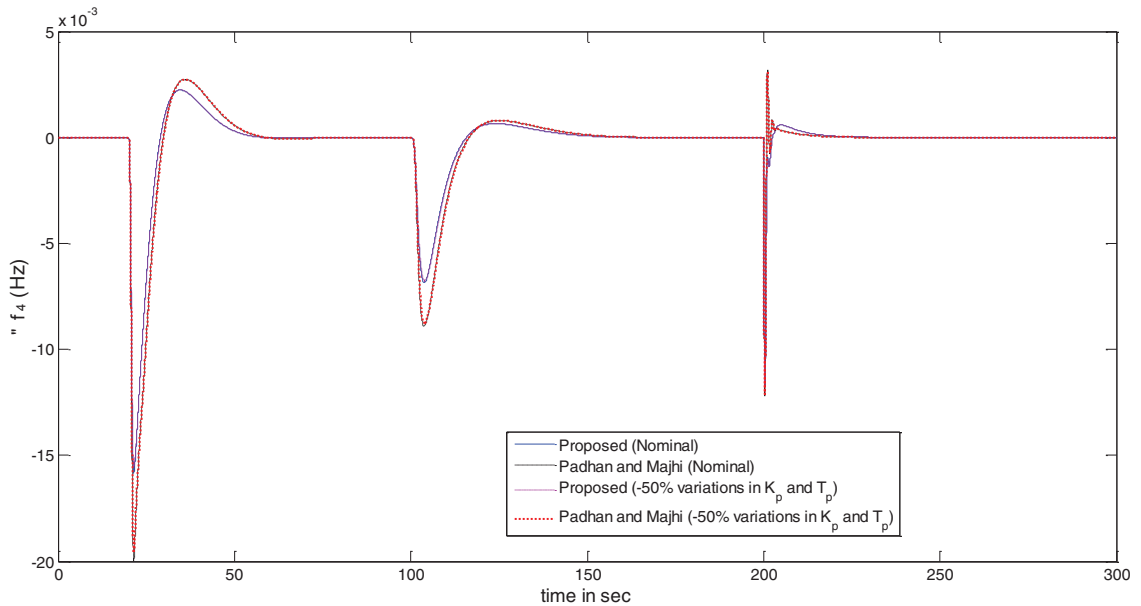


Figure 12 Frequency deviation in area 3 following a small change in loads ΔP_{di} .

Table 3 Controller settings for four area system

Power system	FPD+I settings with GU=10
Area 1,2 and 3	$GP = 0.17, GD = 0.10, GI = 0.85$
Area 4	$GP = 0.20, GD = 0.04, GI = 2.00$

$2.4, T_{r1} = T_{r2} = T_{r3} = 20, c_1 = c_2 = c_3 = 0.333.$

2. Area 4 non-reheated turbine: $K_{P4} = 120, T_{P4} = 20, T_{T4} = 0.3, T_{G4} = 0.08, R_4 = 2.4$
3. Synchronizing constants: $T_{ij} = 0.0707$
4. Frequency bias constants: $B_i = 0.425$

Table 4 shows the proposed hybrid FPD+I controller settings for individual control area. For the same power system

example Padhan and Majhi [15] gave the PID controller settings for area 1, area 2 and area 3 as $K_c = 1.1895, T_i = 1.9090$ and $T_d = 0.5454$ and for area 4 as $K_c = 1.9822, T_i = 0.5242$ and $T_d = 0.1756$.

To prove the effectiveness of the hybrid control scheme, a step load $\Delta P_{d1} = 0.03$ is applied to area 1 at $t = 20$ s, followed by a step load $\Delta P_{d2} = 0.05$ is applied to area 2 at $t = 100$ s, followed by a step load $\Delta P_{d4} = 0.01$ is applied to area 4 at $t = 200$ s. The simulations have been conducted for two types of controllers following small step changes in areas 1, 2 and 4 and the results for frequency changes are shown in Figs. 10 to 13.

The results clearly show the advantage of using the new hybrid FPD+I controller. Upon simulation of the results, it can be observed that the frequency errors and tie-line power

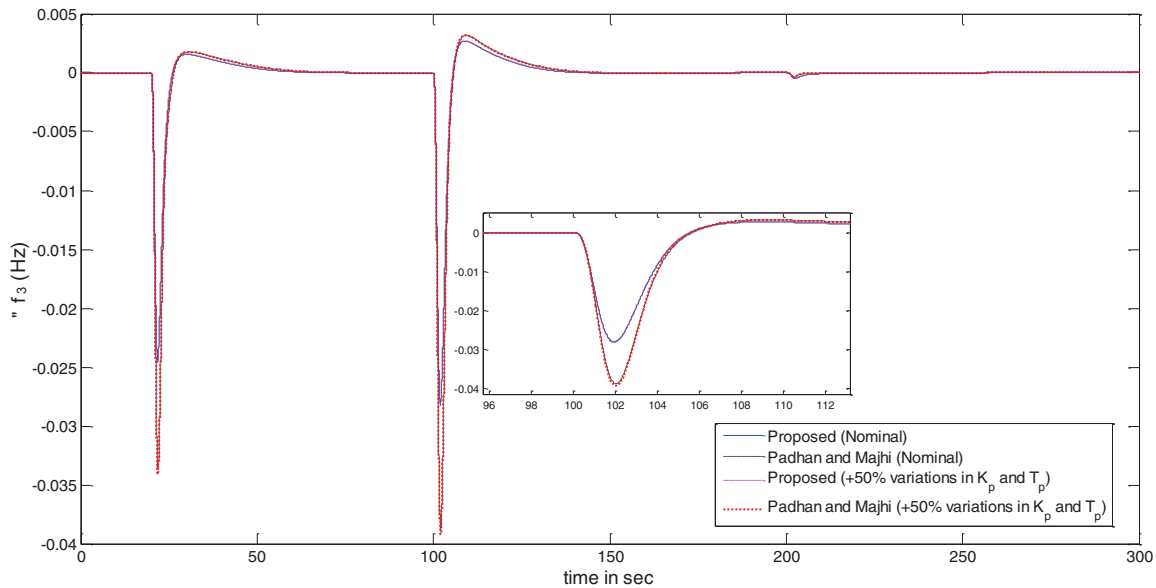


Figure 13 Frequency deviation in area 4 following a small change in loads ΔP_{di} .

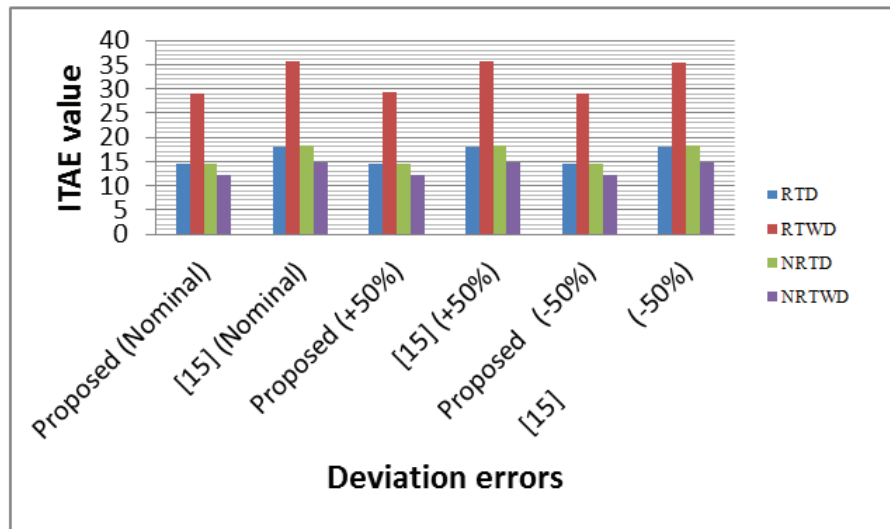


Figure 14 Frequency deviation errors (ITAE) in different areas.

deviations have been driven to zero by means of suggested technique in the occurrences of power load changes.

The stability robustness is also been verified by changing the reheat and non-reheat unit parameters in the 4 areas ($\pm 50\%$ of their nominal values). Nevertheless, the parameters of the controller are unchanged with the system parameter variations. The frequency errors of the 4 areas with the variant parameter values are shown in figures, thus confirming that the passivity is still acceptable for the presented hybrid technique as compared to that with [16].

The frequency deviation in each area is measured using a performance index namely, integral-time-absolute-error (ITAE) criterion. From Fig. 14, it can be revealed that the presented hybrid controller gives less frequency deviations compared to the method in [16] for both nominal and perturbed systems.

6. CONCLUSION

A hybrid configuration for PID type controller has been presented, implemented and examined which will improve the performance of the conventional PID approach. The characteristic of LFC in a single-area power system consisting of reheat and non-reheat turbine has been examined. The designing of the new hybrid controller based on fuzzy logic theory is simple to implement and verify. The results have shown that the suggested design has a better performance and is robust than the recently reported approaches. The new technique is applied to a four-control area power system and verified with various plant parameter uncertainty scenarios. The presented technique has proved to be robust and enhances the damping of the power system following a small step change in load for different cases, hence, provides an improved performance compared to the recently reported methods.

REFERENCES

1. Kundur P. Power system stability and control, TMH, 8th reprint; 2009.
2. Ibraheem, P., Kothari DP. Recent philosophies of automatic generation control strategies in power systems. *IEEE Trans Power Syst* 2005; 20(1):346-57.
3. Sondhi, S. and Hote, V. Fractional order PID controller for load frequency control. *Energy Conversion and Management* 2014; 85: 343-353.
4. Shayeghi H, Shayanfar HA, Jalili A. Load frequency control strategies: a state-of-the-art survey for the researcher. *Energy Convers Manage* 2009; 50:344-53.
5. Rerkpreedapong D, Hasanovic A, Feliachi A. Robust load frequency control using genetic algorithms and linear matrix inequalities. *IEEE Trans Power Syst* 2003; 18(2):855-61.
6. Talaq J, Al-Basri F. Adaptive fuzzy gain scheduling for load frequency control. *IEEE Trans Power Syst* 1999; 14(1):145-50.
7. Juang CF, Lu C-F. Load frequency control by hybrid evolutionary PI controller. *IEE Proc Generat Transm Distrib* 2006; 153(2):196-204.
8. Ali ES, Abd-Elazim SM. Bacteria foraging optimization algorithm based load frequency controller for interconnected power system. *Int J Electr Power Energy Syst* 2011; 33(3):633-638.
9. Mehta, U. and Vachkov, G.: The constraint optimization approach for robust PID design in AVR system, *International Journal of Engineering Intelligent Systems*, vol. 23(1), 2015.
10. Moon YH, Ryu HS, Lee JG, Kim S. Power system load frequency control using noise-tolerable PID feedback. *Proc IEEE Int Symp Ind Electron (ISIE)* 2001; 3:1714-718.
11. Sahib, M. A novel optimal PID plus second order derivative controller for AVR system. *Engineering Science and Technology an International Journal* 2014; 1-13.
12. Mohanty, B., Panda, S. and Hota, P. Differential evolution algorithm based automatic generation control for interconnected power systems with non-linearity. *Alexandria Engineering Journal* 2014; 53: 537-552.
13. Sadaat, H. *Power System Analysis*. Kevin Kane. 1999; p.527-528.
14. Sharma, Y. and Saikia, L. Automatic generation control of a multi-area ST - Thermal power system using Grey Wolf Optimizer algorithm based classical controllers. *Electrical Power and Energy Systems* 2014; 73: 853-862.
15. Tan W. Unified tuning of PID load frequency controller for power systems via IMC. *IEEE Transactions on Power systems* 2010; 25(1):341-350.
16. Padhan, DG. and Majhi, S. A new control scheme for PID load frequency controller of single-area and multi-area power systems. *ISA Transactions* 2012; 52: 242-251.
17. Wang YG., Shao H. Optimal tuning for PI controller. *Automatica*. 2000; 36:147-152.
18. Chang C. Fu W. Area load frequency control using fuzzy gain scheduling of PI controllers. *Electric Power Systems Research*. 1997; 42:145-152.
19. Hosseini S., Etemadi A. Adaptive neuro-fuzzy inference system based auto-matic generation control. *Electric Power Systems Research* 2008; 78:1230-1239.
20. Jantzen, J. Tuning of fuzzy PID controllers. Denmark Tech. Report no 98-H 871 1999; 1-22.
21. Mamdani, E.H. Application of fuzzy algorithms for control of simple dynamic plant. *Proc. Inst. Elect. Eng. Contr. Sci.* 1974; 121: 1585-1588.
22. Takagi T., Sugeno M. Fuzzy identification of systems and its applications to modeling and control. *IEEE Trans. Syst., Man, Cybern* 1985; 15: 116-132.
23. Mann G.K., B.-G. Hu, Gosine R.G. Analysis of direct action fuzzy PID controller structures. *IEEE Trans. Syst., Man, Cybern., Part B* 1999; 29(3): 371-388.
24. Rout U., Sahu R., Panda S. Design and analysis of differential evolution algorithm based automatic generation control for interconnected power system. *Ain Shams Engineering Journal* 2013; 4: 409-421.
25. Khodabakhshian A., Edrisi M. A new robust PID load frequency controller. *Control Engineering Practice* 2008; 16: 1069-1080.
26. Dash P., Saikia L., Sinha N. Automatic generation control of multi area thermal system using Bat algorithm optimized PID cascade controller. *Electrical Power and Energy Systems* 2015; 68: 364-372.
27. Bevrani H. *Robust power system frequency control*. Springer; 2009.

